

## Journal of Nanoscience with Advanced Technology

### Emerging Magnetic Effects of Au Break Junctions with Embedded Ni Nanoparticles

D Deniz, P Gartland\* and D Davidovic

Georgia Institute of Technology

**\*Corresponding author:** Patrick Gartland, Georgia Institute of Technology, School of Physics, 837 State Street, Atlanta, GA 30332, USA; Tel: 404-894-5201; E-mail: pgartland3@gatech.edu

**Article Type:** Research, **Submission Date:** 19 June 2015, **Accepted Date:** 09 July 2015, **Published Date:** 16 July 2015.

**Citation:** D Deniz, P Gartland and D Davidovic (2015) Advances in Analytical Modelling for Nano-Bio-Technology. J Nanosci Adv Tech 1(2): 1-5. doi: <https://doi.org/10.24218/jnat.2015.06>.

**Copyright:** © 2015 P Gartland, et al. This is an open-access article distributed under the terms of the Creative Commons Attribution License, which permits unrestricted use, distribution, and reproduction in any medium, provided the original author and source are credited.

#### Abstract

The technological feasibility of spin valve devices containing ferromagnetic nanoparticles depends on the fabrication of clean ohmic contacts that bridge the region between the particle and external electronics. In this paper we use an electrode-narrowing technique to create oxide free contacts on ferromagnetic nanoparticles embedded under gold nanoconstrictions. Constrictions are narrowed with a feedback-based electromigration method, which reduces the sample conductance to a few multiples of the conductance quantum  $G_0 = 2e^2/h$ . Magnetoresistance measurements show that hysteresis loops emerge as the constriction conductance decreases towards the conductance quantum. The technique can be used to create ohmic contacts to ferromagnetic nanoparticles for spin-based electronics applications.

**Keywords:** Electromigration, Break junction, Ohmic, Magnetic, Nanoparticle

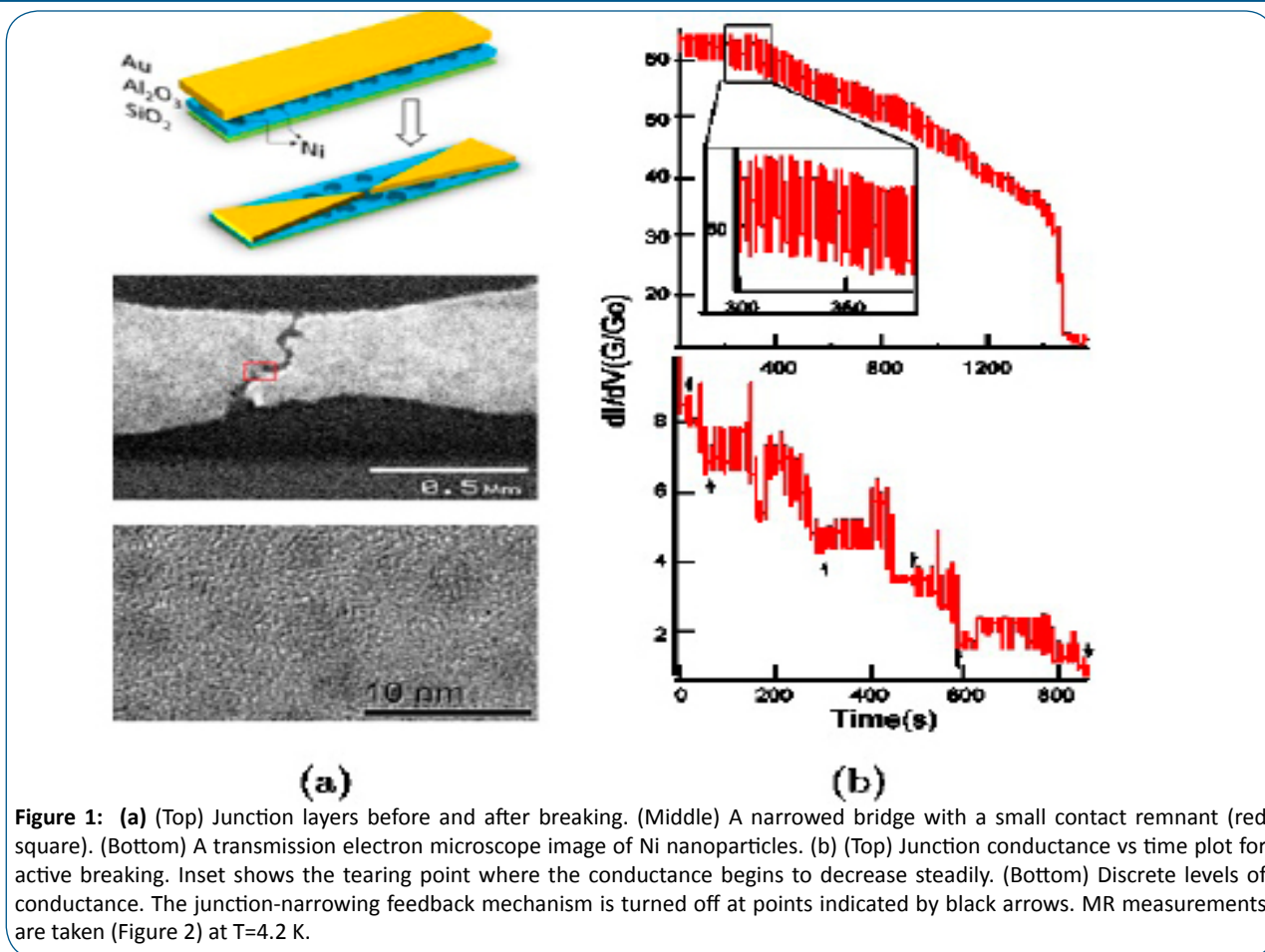
#### Introduction

The magnetization of a ferromagnet in a junction can be controlled by spin-transfer torque (STT) from a spin-polarized current without the need of an external magnetic field [1–4]. STT-induced switching of the particle's magnetization state can be accomplished more efficiently if the inter-electrode junction size can be reduced to the size of the nanoparticle. This switching also depends on the thickness and the material composition of interface layers between the magnetic particle and the control electrodes, and on the level of unwanted surface oxidation [5]. To increase the precision and efficiency of magnetization control, clean ohmic contacts are crucial for practical device applications. One method has shown that electromigration can be used to create clean contacts, even on the single-molecule level [6]. Similarly, single electron transistors have been fabricated using electromigration [7,8]. In this work, we present magnetic field dependence of electron transport through an atomic-scale break junction containing Ni nanoparticles with diameter range 2 to 5 nm, at  $T=4.2$  K [9–11]. Junctions fabricated using the electromigration technique ensure clean contacts to ferromagnetic nanoparticles, and, in principle, nanoparticles in such a device can replace the ferromagnetic layer in a spin-valve or a STT device.

#### Methods

Sample preparation is initiated by electron beam lithography of the bowtie geometry on an insulating  $\text{SiO}_2$  substrate, as indicated in Figure 1. We utilize a JEOL model JSM5910 scanning electron microscope to image and perform lithography. We define and write the sample geometry using a numerical control program called Nanometer Pattern Generation System. The electron-beam resist consists of a polymethylmethacrylate / methylmethacrylate (PMMA/MMA) bilayer. After the electron beam exposure and the development process, we place the sample in a vacuum chamber and evaporate layers of  $\text{Al}_2\text{O}_3$  (5 nm), Ni (1.5 nm) and Au (7 nm) consecutively. The thin layer of Ni nucleates into individual nanoparticles on the amorphous  $\text{Al}_2\text{O}_3$  layer. These particles are embedded within the Au nanoconstriction layer that is deposited on top. Finally, we remove the remaining electron-beam resist and metal layers by a liftoff process in acetone. Because the effectiveness of electromigration depends strongly on the series resistance connected to the device [12], even the large-scale leads' design structure affects the long term fate of break junctions. Therefore, our bow-tie shaped electrode angles ( $\sim 60^\circ$ ) are chosen to have low series resistance. At the narrowest section, these electrodes form a bridge 100 nm wide and 500 nm long. Control samples are fabricated in the same manner, but without a Ni layer.

After the fabrication of Au nanoconstrictions with embedded Ni nanoparticles, the experimental procedure consists of two main parts. First, we use a feedback-based electromigration technique to narrow the junctions. Second, we perform magnetoresistance (MR) measurements of the junctions at a small, fixed bias voltage by sweeping a magnetic field in a triangle wave. Electromigration is the process by which linear momentum is transferred from electrons to metal ions, and can cause the drift and restructuring of metal ions in nanoconstrictions. During the feedback-based junction narrowing process, when the conductance falls below  $10 G_0$ , we halt the narrowing process and measure the MR. This procedure enables us to check whether contacts on Ni nanoparticles are formed, by observing any emerging magnetic reactions at different levels of conductance. We also use conductance histogram comparisons of narrowed devices with and without Ni nanoparticles as a supplementary tool to check occurrence of contacts on ferromagnetic nanoparticles. Slight



shifts of the time-histogram conductance peaks can result from additional resistance due to the presence of a Ni nanoparticle, rather than a Au cluster, in the junction.

Electromigration has long been used to break gold wires in a controlled way [13]. One of the most common feedback techniques, active breaking [14,15], is used in this experiment with few modifications to a previously studied method [16]. Resistance values of the junction are monitored by applying a bias voltage and measuring the voltage difference across and current through the junction with National Instruments data acquisition board at an adjustable sampling period,  $T_R$ , which we initialize to 30 ms. The junction current is kept below 10 mA at all times, and is measured by an Ithaco current amplifier. If the resistance remains below a previously set threshold parameter,  $R_{max}$ , then the voltage is ramped from 100 mV in steps of 4 mV per loop iteration. Initially, the junction resistance is on the order of 200  $\Omega$ .  $R_{max}$  is updated recursively after each loop iteration by adding a certain percentage of the initial resistance to itself. At the early stages of the experiment, this percentage is kept at 1% of the resistance calculated at the beginning of the loop. As the conductance is reduced to couple multiples of  $G_0$ , this percentage is increased up to 10%. If the resistance exceeds  $R_{max}$ , then the voltage is reduced to its minimum value of 100 mV. This procedure creates an oscillation in the plot of  $dI/dV$  vs time, and the two parameters,  $T_R$  and  $R_{max}$ , are updated in a controlled way to increase oscillation amplitude until the moving average of the differential conductance value starts to decrease. We denote this sudden drop in the moving average of junction conductance as the tearing point of the junction, and display data

of such an event in a representative sample in the inset of Figure 1(b). After the tearing point,  $T_R$  and  $R_{max}$  are altered to induce a smooth transition to lower conductance levels. Sampling time is varied from 30 ms to 10 ms during the process in order to adjust the narrowing rate. Even though this slows down the whole narrowing process, it decreases the probability of sudden breaking by enabling the time required to respond and change  $R_{max}$ . It also increases the accuracy to reach a target resistance by creating more feedback time to react to any upcoming changes in resistance.

Samples are narrowed down to different conduction levels (Figure 1(b), (bottom)) and MR measurements are performed. We expect that the junction breaks due to the migration of Au atoms, rather than Ni. The current density will be higher in Au than in Ni particles, because the conductivity of Au is larger than in Ni, and because of the electron scattering at the Ni-Au interface. The larger current density in Au increases the strength of electromigration in Au. In addition, the larger mobility of Au relative to Ni will also promote greater relative electromigration in Au. The mobility of ions in electromigration is dominated by the interaction of atoms with their surroundings in their bulk forms. This interaction is independent of ion's mass. For example, copper is one of the few other metals that is susceptible to electromigration, and although copper has smaller ion mass than that of gold, copper needs current densities orders of magnitude higher for electromigration to occur [17]. Additionally, the probability of having contacts involving the Ni nanoparticle will increase with the nanoparticle size and its volume fraction in the film. Therefore, in order to increase the odds of nanoparticle-

mediated transport in the narrowed junctions, our experiment include a 1.5 nm Ni layer, which causes nucleation of Ni in the form of nanoparticles, as seen in the Transmission Electron Microscope image in Figure 1(a)(bottom).

Samples are connected electrically to a probe we custom-built in our lab. Within the probe is a solenoid utilized for the superconducting magnet. The entire probe apparatus is submerged in a liquid helium dewar, in order to maintain temperatures of 4.2K. The temperature can be monitored by using a calibrated resistor.

### Experimental Results and Discussion

In Figure 2(a), no MR at  $8.5G_0$  confirms that most of the conduction is through the Au layer, rather than through Ni particles. A distinguishable MR effect appears once the conductance is decreased to  $4.6G_0$ . At this level of conductance, hysteresis loops also emerge for the first time. As the conductance is decreased, the same percentage of MR is observed for narrower junctions, even though the amount of current going through the junction is reduced ( $3\mu\text{A}$  for (a),  $1\mu\text{A}$  for (b),  $500\text{nA}$  for (c), and  $320\text{nA}$  for (d)) every time the junction is narrowed. In Figure 2(d), hysteresis loops are not visible in the averaged data. However, a closer look at the raw data of current vs magnetic field, as shown in Figure 3, reveals that conduction is occurring through at least two metastable conduction levels, which hides observation of hysteresis loops with the switching field around  $\pm 50\text{ mT}$ . It may be noted that the hysteresis loops change qualitatively as a function of conductance. That is, the resistance valley in Figure 2(b) and 2(c) lie on inverted sides of zero magnetic field. This could be a consequence of the influence of one or multiple secondary Ni particles in the vicinity of the particle involved in transport, which may alter the primary Ni particle's magnetization due to

magnetostatic dipole fields in opposition to the applied field. As the conductance changes, so too does the geometric structure of the junction as the ions move due to electromigration. As this occurs, the Au atoms could displace the secondary Ni particle enough to remove its influence on the primary Ni particle subject to electron transport. While a full explanation of the effect is beyond the present scope, it hints at the complexity of the junction rearrangement process in electromigration, and could be a promising avenue for further study. The main result of this work, however, holds regardless of such effects. That is, MR emerges as the conductance levels drop in our nanoconstriction junctions.

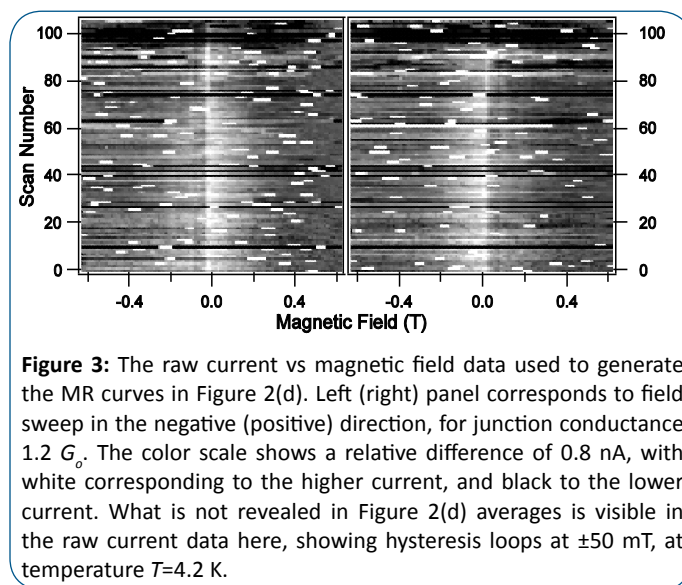


**Figure 3:** The raw current vs magnetic field data used to generate the MR curves in Figure 2(d). Left (right) panel corresponds to field sweep in the negative (positive) direction, for junction conductance  $1.2 G_0$ . The color scale shows a relative difference of  $0.8\text{ nA}$ , with white corresponding to the higher current, and black to the lower current. What is not revealed in Figure 2(d) averages is visible in the raw current data here, showing hysteresis loops at  $\pm 50\text{ mT}$ , at temperature  $T=4.2\text{ K}$ .

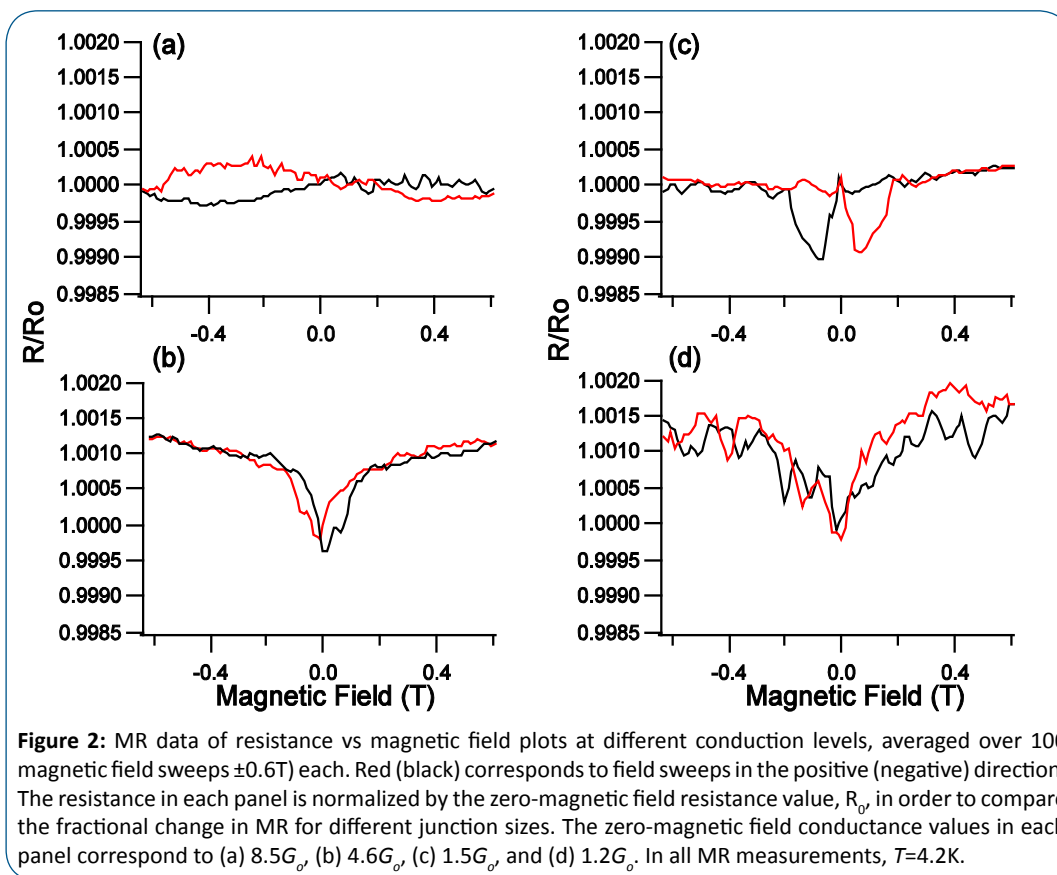


**Figure 2:** MR data of resistance vs magnetic field plots at different conduction levels, averaged over 100 magnetic field sweeps  $\pm 0.6\text{ T}$  each. Red (black) corresponds to field sweeps in the positive (negative) direction. The resistance in each panel is normalized by the zero-magnetic field resistance value,  $R_0$ , in order to compare the fractional change in MR for different junction sizes. The zero-magnetic field conductance values in each panel correspond to (a)  $8.5G_0$ , (b)  $4.6G_0$ , (c)  $1.5G_0$ , and (d)  $1.2G_0$ . In all MR measurements,  $T=4.2\text{ K}$ .

Another way to verify the conduction through nanoparticles is the method of conductance histograms. Conduction quantization in gold chains is observed to be integer multiples of  $G_0$  [18]. Two-dimensional (2D) bridges can have complicated structural arrangements for multi-channel transport [19]. For the case of breaking of 2D gold nanoconstrictions, O'Neill et al [16] observed non-integer values in their conductance histograms. Their histograms were collected during the self-breaking of gold nanoconstrictions. We used this method with the assumption that having Ni nanoparticles under narrowed gold nanoconstrictions should cause additional resistance due to additional scattering from a structural change in the bridge. Such an effect should be visible predominantly in smaller levels of conduction due to the size of our particles. Therefore, we first collect self-breaking data of five control-sample Au nanoconstrictions, which do not contain Ni nanoparticles and combine them in a conductance histogram as measured over time. Next, we compare this histogram to the histogram of a Ni-containing device. But, since the narrowest area of a breaking junction may or may not contain a Ni nanoparticle, we only choose the histograms of devices which showed emergent magnetic behavior. In other words, we choose only those devices that already showed a MR-clue of having a Ni nanoparticle in the junction. When this comparison is made, as seen in Figure 4, we see a slight shift to the left in the conduction histogram of the Ni nanoparticle devices, compared to the combined histogram of devices without Ni nanoparticles.

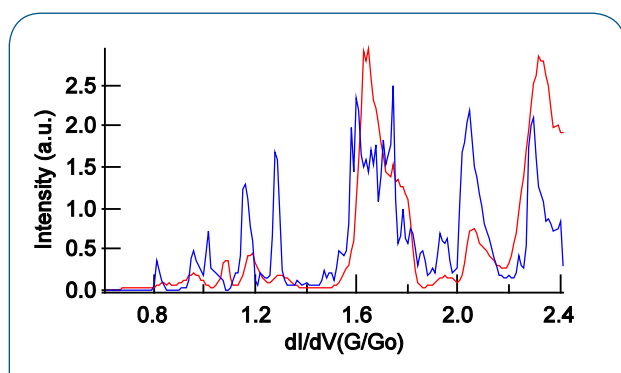


**Figure 4:** Conductance histograms of self breaking of five nanoconstrictions that do not contain Ni nanoparticles (red) vs histograms of the Ni nanoparticle containing device that showed emergent magnetic behavior (Figure 2). A slight shift in the blue curve results from additional resistance due to a nanoparticle connection at the narrowest part of the junction which causes a structural change.

## Conclusion

Emergent magnetic behavior in narrowed junctions, along with a shift in conductance histograms indicate that the presented technique can be used to create ohmic contacts to ferromagnetic nanoparticles. These contact areas are free of oxides, which is an important feature for the quality of magnetic switching signals. The technique can also be used to develop nanoparticle-embedded spin-valve and STT device designs, where a ferromagnetic layer is replaced by a ferromagnetic nanoparticle.

## Acknowledgements

This work has been supported by the Department of Energy (DE-FG02-06ER46281).

## References

1. Sankey JC, Cui YT, Sun JZ, Slonczewski JC, Buhrman RA, Ralph DC. Measurement of the spin-transfer torque vector in magnetic tunnel junctions. *Nature Physics*. 2008; 4:67–71. doi:10.1038/nphys783.
2. Ralph D, Stiles M. Spin transfer torques. *Journal of Magnetism and Magnetic Materials*. 2008; 320(7):1190 – 1216. doi:10.1016/j.jmmm.2007.12.019.
3. Katine J, Albert F, Buhrman R, Myers E, Ralph D. Current-driven magnetization reversal and spin-wave excitations in Co/Cu/Co pillars. *Phys. Rev. Lett*. 2000; 84:3149. doi: <http://dx.doi.org/10.1103/PhysRevLett.84.3149>.
4. Slonczewski JC. Current-driven excitation of magnetic multilayers. *Journal of Magnetism and Magnetic Materials*. 1996; 159(1-2):L1–L7. doi:10.1016/0304-8853(96)00062-5.
5. Cobas E, Friedman AL, van Erve OM, Robinson JT, Jonker BT. Graphene as a tunnel barrier: graphene-based magnetic tunnel junctions. *Nano Lett*. 2012; 12(6):3000–3004. doi: 10.1021/nl3007616.
6. Burzurı E, Zyazin AS, Cornia A, van der Zant HSJ. Direct observation of magnetic anisotropy in an individual fe4 single-molecule magnet. *Phys Rev Lett*. 2012; 109(14):147203.
7. Bolotin KI, Kuemmeth F, Pasupathy A, Ralph D. Metal-nanoparticle single-electron transistors fabricated using electromigration. *Appl. Phys. Lett*. 2004; 84:3154–3156. doi: <http://dx.doi.org/10.1063/1.1695203>.
8. Park H, Park J, Lim AK, Anderson EH, Alivisatos AP, McEuen PL. Nanomechanical oscillations in a single-c60 transistor. *Nature*. 2000; 407:57–60. doi:10.1038/35024031.
9. Jiang W, Gartland P, Davidovic D. Size-dependence of magneto-electronic coupling in Co nanoparticles. *J. Appl. Phys*. 2013; 113:223703. doi: <http://dx.doi.org/10.1063/1.4810853>.
10. Strachan DR, Smith DE, Fischbein MD, Johnston DE, Guiton BS, Drndic M, et al. Clean electromigrated nanogaps imaged by transmission electron microscopy. *Nano Lett*. 2006; 6(3):441–444.
11. Khondaker SI, Yao Z. Fabrication of nanometer-spaced electrodes using gold nanoparticles. *Applied Physics Letters*. 2002; 81:4613–4615.
12. Taychatanapat T, Bolotin KI, Kuemmeth F, Ralph DC. Imaging electromigration during the formation of break junctions. *Nano Lett*. 2007; 7(3):652–656.
13. Park H, Lim AK, Alivisatos AP, Park J, McEuen PL. Fabrication of metallic electrodes with nanometer separation by electromigration. *Appl. Phys. Lett*. 1999; 75:301–303. doi: <http://dx.doi.org/10.1063/1.124354>.
14. Strachan D, Smith D, Johnston D, Park TH, Therien MJ, Bonnell D, et al. Controlled fabrication of nanogaps in ambient environment for molecular electronics. *Appl. Phys. Lett*. 2005; 86:043109. doi: <http://dx.doi.org/10.1063/1.1857095>.
15. Van der Zant HS, Groot Z, Van Walree CA, Yann-Vai Kervennic, Menno Poot, Kevin O’Neill, et al. Molecular three-terminal devices: fabrication and measurements. *Faraday Discussions*. 2006; 131:347–356. doi: 10.1039/B506240N.
16. O'Neill K, Osorio E, Van der Zant H. Self-breaking in planar few-atom Au constrictions for nanometer-spaced electrodes. *Appl. Phys. Lett*. 2007; 90:133109. doi: <http://dx.doi.org/10.1063/1.2716989>.
17. Lloyd JR, Clement JJ. Electromigration in copper conductors. *Thin solid films*. 1995; 262(1-2):135–141. doi:10.1016/0040-6090(94)05806-7.

18. Ohnishi H, Kondo Y, Takayanagi K. Quantized conductance through individual rows of suspended gold atoms. *Nature*. 1998; 395:780–783. doi:10.1038/27399.
19. Ferry DK, Goodnick SM. *Transport in nanostructures*. Cambridge: Cambridge University Press; 1997. p. 128–131.